6th European Conference on Computational Mechanics (ECCM 6)
7th European Conference on Computational Fluid Dynamics (ECFD 7)
11 – 15 June 2018, Glasgow, UK

NUMERICAL SIMULATION OF FLUID STRUCTURE INTERACTION IN A PUMP WITH HYPERELASTIC COMPONENTS

CHRISTIAN ZEHETNER[1,2], FRANZ HAMMELMÜLLER[2] AND CHRISTIAN WÖCKINGER[3]

[1]University of Applied Sciences Upper Austria
Stelzhamerstr. 23, 4600 Wels, Austria
christian.zehetner@fh-wels.at, www.fh-ooe.at

[2]Linz Center of Mechatronics GmbH
Altenbergerstr. 69, 4040 Linz, Austria
franz.hammelmueller@lcm.at, www.lcm.at

[3] Primetals Technologies Austria GmbH
Turmstr. 44, 4031 Linz, Austria
christian.woeckinger@primetals.com, www.primetals.com

Key words: Fluid Structure Interaction, SPH, Hyperelasticity, Pump

Abstract. Interaction of fluids with structures play an important role in many industrial applications, e.g. in pumps as major components of conveying processes. This paper concerns the numerical analysis of fluid structure interaction in a pump. The considered system consists of a metal housing, a polymer impeller and the fluid. Thus, we deal with several non-linearities: large strains, nonlinear material behavior and contact. To analyze this pump, Finite Element Method (FEM) and Smoothed Particle Hydrodynamics (SPH) are coupled, both methods are Lagrangian formulations. Numerical results are presented and discussed. The present study is a benchmark for the analysis of fluid structure interaction with highly nonlinear components. The results show that the presented simulation strategy is suitable for the optimization of such kinds of industrial problems.

1 INTRODUCTION

Fluid-structure interaction (FSI) occurs in many industrial applications, in which fluid flow and flexible deformations of solid structures are coupled. Examples are obstacles in fluid flow, the dynamics of fluid-filled structures or transport problems. Efficient numerical strategies are required to optimize such kinds of problems.

Very important components in many industrial applications are pumps to convey matter like water, oil, food, granulate etc. There exist many different concepts for pumps, the benefits of the respective type depend on the goods to be conveyed, the specific task and costs. Here, we consider a radial pump with a housing of metal and a polymer impeller. After installing the impeller into the pump its blades highly deform, as shown in Figure 1. Utilizing this elasticity, a good sealing can be achieved. Moreover, noise can be reduced by using a soft impeller. Depending on the type of fluid to be transported, the material of the impeller must

be chosen accordingly. E.g., for transport of food, chloroprene, also known as neoprene is frequently used.

Goal of this work is to develop an efficient simulation model for such kinds of problems, which can subsequently be used for optimizing these components in industrial applications.

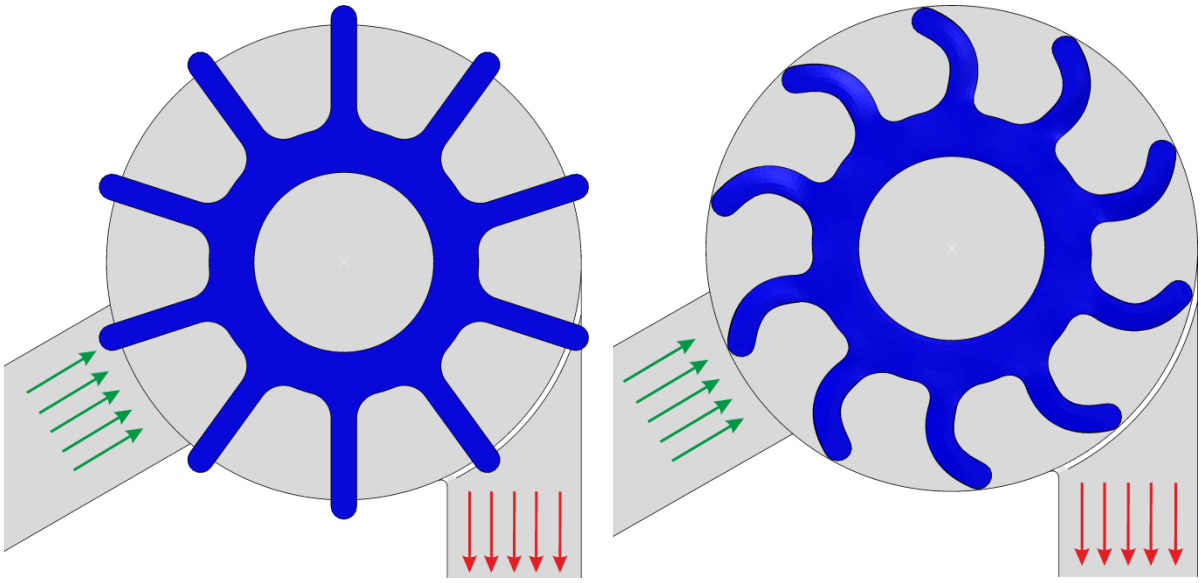

Figure 1: Impeller and deformed impeller in the pump

For simulating and optimizing such pumps in operation there are different numerical strategies: One possibility is a Coupled Eulerian Lagrangian analysis, CEL, [1]. In such an analysis, the solid bodies are represented by Lagrangian Finite Elements, and the fluid by Eulerian Finite Volumes. Another numerical method to model FSI is to couple Lagrangian Finite Method (FEM) with Smoothed Particle Hydrodynamics, SPH, [2]. The latter is a meshfree Lagrangian formulation, suitable for analysing fluid flow and large deformations of solids. The advantage of a coupled FEM-SPH analysis compared to a CEL analysis in FSI problems is the Lagrangian formulation for the solids and the fluid, which frequently is numerically more efficient and robust compared to the Eulerian formulation. In a former study, [3], this benefit has been demonstrated by comparing FEM-SPH and CEL for the example of a fluid filled container colliding with a wall: The computation time of the SPH model has been half of the CEL model. Therefore, the coupled FEM-SPH analysis has been chosen for the investigations in this paper.

In the following, the simulation model for a pump with a metal housing, a neoprene impeller and fluid is discussed. The complexity of this problem is high because we consider the large deformation of the impeller, its highly nonlinear hyperelastic material behaviour, fluid flow and the coupling with the flexible structure. Finally, numerical results obtained by ABAQUS are presented showing that the chosen method is suitable for the analysis and optimization of such problems in industrial applications.

2 SIMULATION MODEL

2.1 Components and constitutive relations

The simulation model consists of three parts: Housing, impeller and fluid. The metal housing is assumed to be much stiffer than the polymer impeller and is thus considered as a rigid body, discretized by rigid Finite Elements.

As fluid we consider water with the dynamic viscosity $\eta = 1 \cdot 10^{-9}$ Ns/mm² and density $\rho = 1$ kg/dm³. The speed of sound is set to $c_0 = 1.484 \cdot 10^6$ mm/s. For the water we use smoothed particles. With ABAQUS, a very comfortable definition of the particles is possible: First the fluid domain is discretized by 3D Finite Elements, and then ABAQUS computes the particles automatically according to the defined numerical parameters like number of particles per volume, kernel function, smoothing parameters, etc.

The impeller is a solid body and discretized by solid 3D Finite Elements. The material behavior is represented by a hyperelastic model, viscoelastic behavior is not considered for the first step. In problems involving large deformations, contact and hyperelastic behavior the configuration of the Finite Element mesh plays an important role to obtain reliable results, i.e. a good convergence with reasonable computation time. Usually, in case of complicated geometry, large effort must be spent to define a mesh consisting mostly of hexahedral elements in the regions of critical stress and strains. Here, we deal with a quite simple geometry for which Figure 2 shows the mesh of the undeformed impeller and the housing.

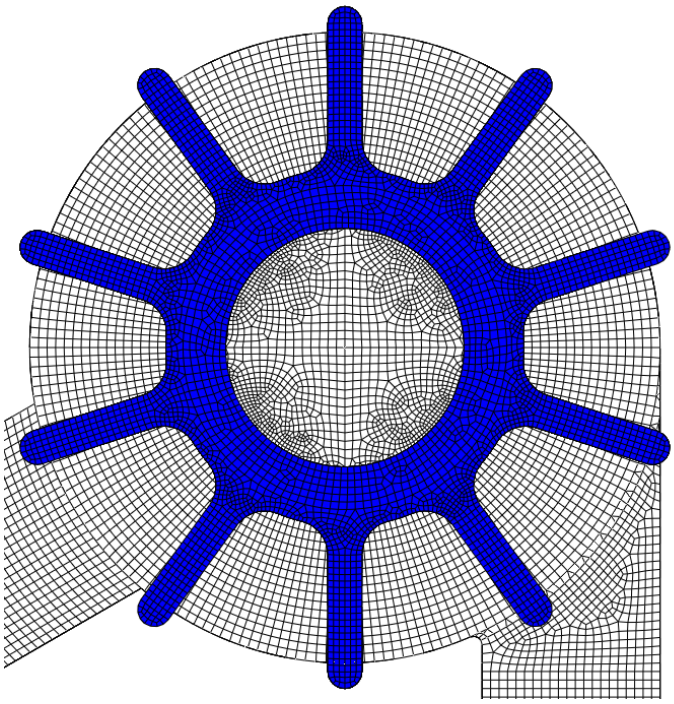

Figure 2: Mesh of undeformed impeller and housing

The behavior of polymers highly depends on the specific composition. Here, we use an Ogden model of order three. In this model, the Helmholtz strain energy function is expressed

in terms of principal stretches $\lambda_1, \lambda_2, \lambda_3$. The square of the principle stretches, λ_i^2, are the eigenvalues of the Cauchy-Green strain tensor $\boldsymbol{C}$. The stress components are subsequently derived from the strain energy function. For modelling hyperelastic materials like neoprene it is suitable to decompose the strain energy function into an isochoric and volumetric part because the volumetric stiffness is much higher than the shear stiffness, cf Holzapfel [4]. According to ABAQUS documentation [5], the Ogden strain energy function is expressed as

$$\Psi = \sum_{i=1}^{3} \frac{2\mu_i}{\alpha_i^2}\left(\bar{\lambda}_1^{\alpha_i} + \bar{\lambda}_2^{\alpha_i} + \bar{\lambda}_3^{\alpha_i} - 3\right) + \sum_{i=1}^{3} \frac{1}{D_i}(J-1)^{2i}, \tag{1}$$

where $\bar{\lambda}_1, \bar{\lambda}_2, \bar{\lambda}_3$ are the deviatoric principal stretches $\bar{\lambda}_i = J^{-1/3}\lambda_i$, and J is the volume ratio, $J = \lambda_1\lambda_2\lambda_3$. The parameters μ_i, α_i and D_i are material coefficients, such that the initial shear modulus is $\mu_0 = \sum_{i=1}^{3} \mu_i$ and the initial bulk modulus is $K_0 = 2/D_1$. Note, that the squares of the modified principal stretches, $\bar{\lambda}_i^2$, are the eigenvalues of the modified Cauchy-Green tensor $\overline{\boldsymbol{C}} = J^{2/3}\boldsymbol{C}$, representing the deviatoric part of strain, i.e. $\bar{\lambda}_1\bar{\lambda}_2\bar{\lambda}_3 = 1$.

Usually, material tests must be performed to obtain the material properties. In this theoretical study we use a parameter set provided by an industrial partner in a former study:

$$\begin{gathered} \alpha_1 = -4.101, \;\; \alpha_2 = 6.254, \;\; \alpha_3 = 1.091, \\ \mu_1 = 0.0743, \;\; \mu_2 = 0.01168, \;\; \mu_3 = 1.3793, \\ D_1 = D_2 = D_3 = 0.001. \end{gathered} \tag{2}$$

To investigate this constitutive behavior for the basic load cases of uniaxial and biaxial tension, we use the assumption of an almost incompressible material, which is a good approximation for many polymers like neoprene. In case of incompressibility the volume ratio is $J = \lambda_1\lambda_2\lambda_3 = 1$, and the strain energy function reduces to

$$\Psi = \sum_{i=1}^{3} \frac{2\mu_i}{\alpha_i^2}\left(\lambda_1^{\alpha_i} + \lambda_2^{\alpha_i} + \lambda_3^{\alpha_i} - 3\right). \tag{3}$$

The principal values of Cauchy stress are derived from this energy potential and can be expressed as a function of the principal stretches as, cf Holzapfel [4],

$$\sigma_i = \lambda_i \frac{\partial \Psi}{\partial \lambda_i} - p, \tag{4}$$

with the hydrostatic pressure p. In this formulation, pressure p is a Lagrangian multiplier and follows from the condition of incompressibility, $\lambda_1\lambda_2\lambda_3 = 1$.

For uniaxial tension, i.e. $\lambda_1 = \lambda, \lambda_2 = \lambda_3 = \lambda^{-1/2}, \sigma = \sigma_1, \sigma_2 = \sigma_3 = 0$, we obtain

$$\sigma = \sum_{i=1}^{3} \frac{2\mu_i}{\alpha_i}\left(\lambda^{\alpha_i} - \lambda^{-\alpha_i/2}\right), \tag{5}$$

and for the case of biaxial tension, i.e. $\lambda_1 = \lambda_2 = \lambda, \lambda_3 = \lambda^{-2}, \sigma = \sigma_1 = \sigma_2, \sigma_3 = 0$,

$$\sigma = \sum_{i=1}^{3} \frac{2\mu_i}{\alpha_i}\left(\lambda^{\alpha_i} - \lambda^{-2\alpha_i}\right). \tag{6}$$

Note, that Ogden-type models are implemented in most Finite Element codes providing the

ability to model hyperelasticity. One of the major benefits of this material law is the relative simple determination of the parameters from a uniaxial tension test.

Using the numerical values in Eq. (2) we obtain the constitutive relations as shown in Figure 3. The left diagram shows Cauchy stress as a function of stretch and the right diagram Cauchy stress as a function of Hencky strain, which is the output variable in the subsequent Finite Element results. Note that for the considered impeller the expected order of magnitude for the maximum stretch is 50%, i.e. $\lambda_{max} \sim 1.5$.

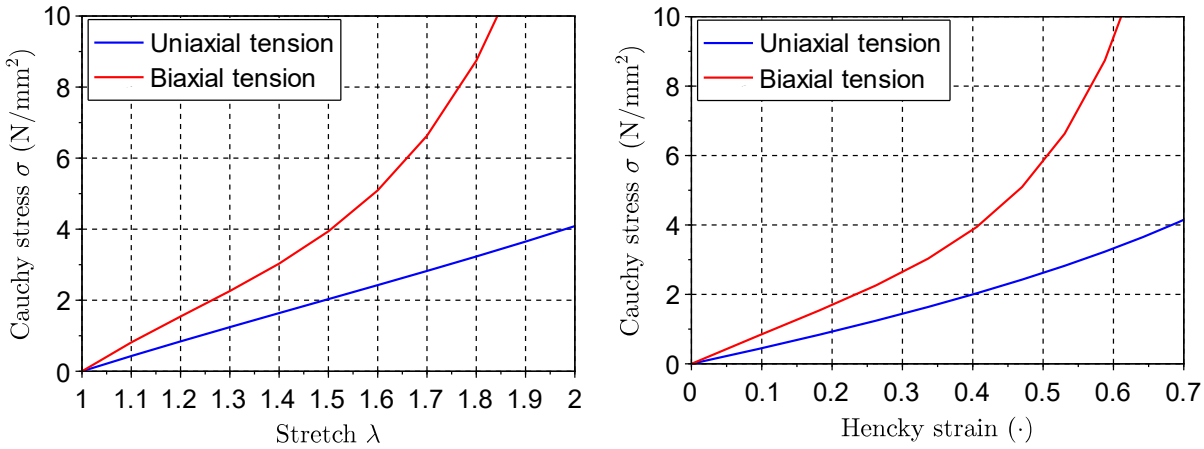

Figure 3: Cauchy stress for uniaxial and biaxial tension as a function of stretch (a) and Hencky strain (b)

The interactions between the components of the pump are defined by a general contact model based on a penalty formulation, refer to ABAQUS online documentation [5] for more details. This kind of contact formulation is very efficient in the present situation, in which we deal with a high number of particles as well as contact closings and openings.

For the simulation of the pump we first need to press the impeller into the housing as shown in Figure 1. In this first step, fluid flow is not yet considered, the impeller is fixed, and contact between blades and housing is not yet defined. The blades are deformed by kinematical boundary conditions, until they are inside the housing. In a second step, the boundary conditions between housing and impeller are defined and the kinematical boundary conditions of the blades are removed. Moreover, the rotation is activated by prescribing the angular velocity (ω=100 rad/s). The motion of the fluid is prescribed by a pressure boundary condition at the inlet. For the simulations the explicit solver of ABAQUS has been used.

3 NUMERICAL RESULTS

From the engineering point of view, the most interesting results are the distributions and maximum values for stress, strain and contact pressure between housing and impeller blades. Because of lifetime, the stress must not exceed a limit value. On the other hand, the contact pressure must be high enough for an appropriate sealing and to avoid leakage. Moreover, fluid flow is interesting because of the performance and efficiency of the pump. In the following, exemplary results are presented for these quantities.

3.1 Stress and strain in the impeller after installing it into the housing

The first interesting results are the stress and strain distributions in the impeller after installing it into the housing. Figure 4 shows the v. Mises stress field. As expected, the maximum stress (1.45 N/mm²) is near the maximum curvature. Figure 5 shows the Hencky strain field, the maximum value is about 0.32, such that the maximum stretch is about 37%. Note that the deformation of the blade is like the bending of a beam. Thus, the state of stress is rather like the uniaxial case in Figure 3 than the biaxial one.

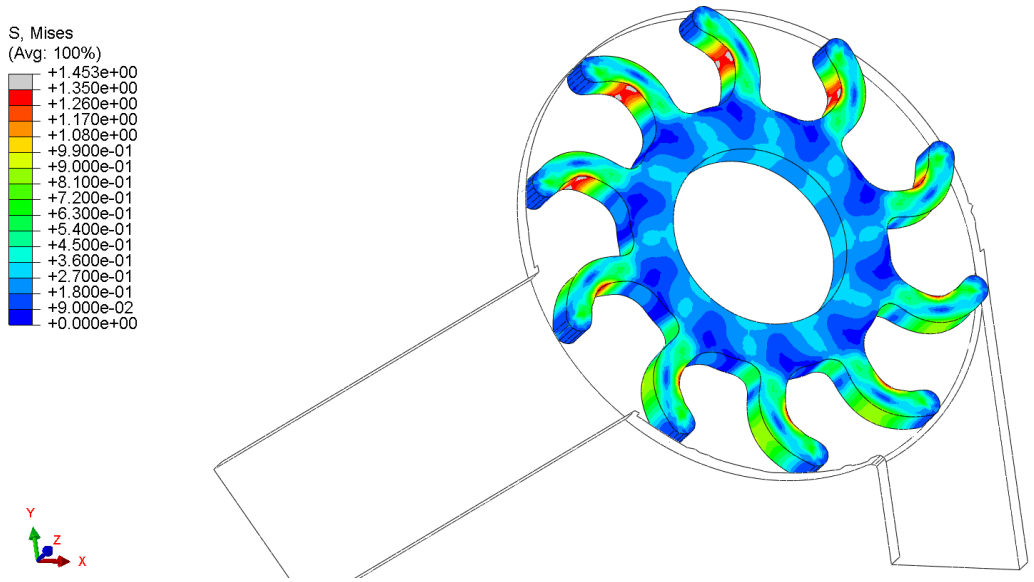

Figure 4: Stress field (v.Mises) of the impeller after installing into the housing (without fluid flow)

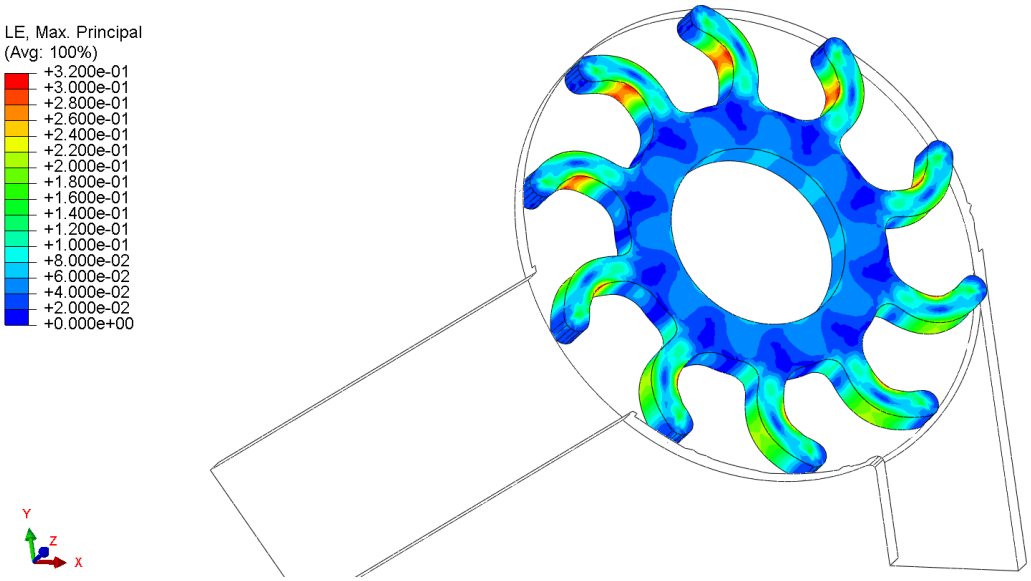

Figure 5: Hencky strain field after installing into the housing (with fluid flow)

3.2 Fluid transport

Secondly, the interaction with the fluid is studied. Figure 6 shows the distribution of the Hencky strain in the impeller and the distribution of the fluid particles. It is obvious that centrifugal forces cause a concentration of the fluid near the wall of the housing. Figure 7 shows the velocity field of impeller and fluid. We also see the acceleration of the fluid: The velocity of the fluid is rising near the outlet.

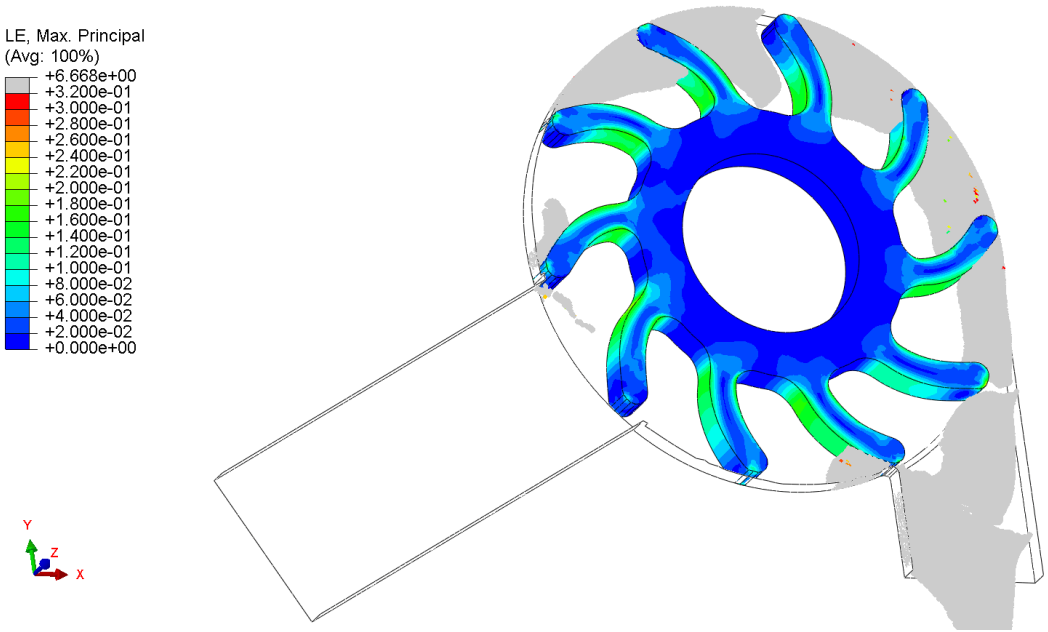

Figure 6: Hencky strain in the impeller and fluid particles

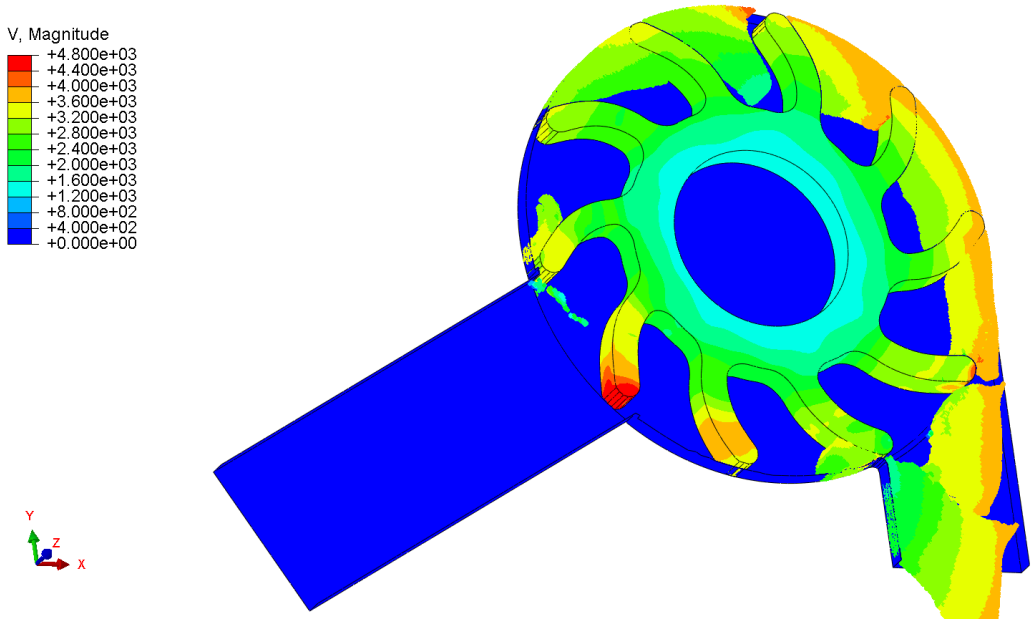

Figure 7: Velocity field of impeller and fluid

3.3. Contact pressure

Finally, the contact pressure between impeller and housing is shown in Figure 8. A sufficient level of contact pressure is necessary for sealing and to avoid leakage. Figure 8 shows that there is a homogeneous distribution of contact pressure for the radial contact surfaces, and that there are regions at the axial contact surfaces without contact pressure, i.e. contact openings. These clearances cause leakage and must be avoided. A possible solution is to add some material in these regions, so that the axial dimension of the impeller is slightly larger than this dimension of the housing. Then, contact pressure is achieved due to the compression of the impeller after installation into the housing.

On the other hand, there are some regions of high contact pressure, represented by gray color. The high pressure is a consequence of the axial extension of the blades in the regions of radial compression due to bending of the blades. In contrast, on the back side of the blades there are radial tensile strains, and axial compressive strains cause a contact opening. Again, the distribution of the contact pressure may be optimized by an appropriate shape of the impeller: Removal of material in the regions of too high pressure and addition of material in the regions of contact opening. This optimization could be topic for a subsequent study.

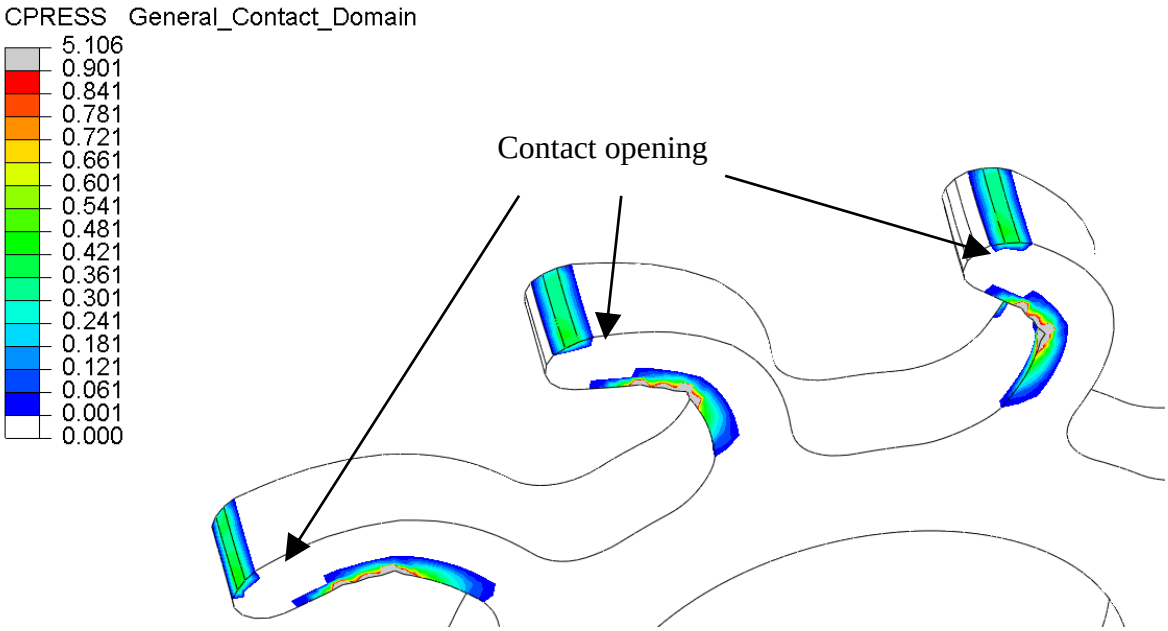

Figure 8: Contact pressure

4 CONCLUSIONS

It has been shown that it is possible to simulate the fluid convey in a pump with a hyperelastic impeller. The complexity of the problem is very high due to several severe nonlinearities. Thus, the computation time is also quite high. During the modelling phase, special care has been taken for generating a high-quality mesh. Once more, it has also turned

out that the mesh quality is one of the most essential aspect for problems including large deformations, high material nonlinearity and contact. Finally, with the appropriate mesh, the simulations have run very robust. For the presented example, physically plausible results have been obtained for answering important engineering questions: Stress, strain, contact pressure, flow velocity etc. The results also show smooth results for the distribution of these quantities. Finally, an optimization of the contact pressure distribution has been suggested by geometric adaptations of the impeller. All in all, the study shows that it is possible to analyze and optimize industrial problems with the presented strategy.

ACKNOWLEDGEMENT

This work has been supported by the COMET-K2 “Center for Symbiotic Mechatronics” of the Linz Center of Mechatronics (LCM) funded by the Austrian federal government and the federal state of Upper Austria.

REFERENCES

[1] D.J. Benson, Computational Methods in Lagrangian and Eulerian Hydrocodes, *Comput. Methods Appl. Mech. Engrg.*, Vol. 99, pp. 235–394, 1992.

[2] J.J. Monaghan, Smoothed Particle Hydrodynamics, *Rep. Prog. Phys*., Vol. 68, pp. 1703–1759, 2005.

[3] C. Zehetner, M. Schörgenhumer, F. Hammelmüller, and A. Humer, Comparison of coupled Euler-Lagrange and Smoothed Particle Hydrodynamics in Fluid-Structure Interaction, *Proceedings of the VI International Conference on Computational Methods for Coupled Problems in Science and Engineering*, COUPLED PROBLEMS 2015, May 18-20, Venice, Italy, 2015, pp. 1080–1088.

[4] G. Holzapfel, Nonlinear Solid Mechanics: A Continuum Approach for Engineering, Wiley, 2000.

[5] ABAQUS 2017 Documentation, *www.3ds.com*